

Measuring Rainfall at Sea.

Part II. Spaceborne sensors

G.D. Quartly, T.H. Guymer and M.A. Srokosz

Southampton Oceanography Centre

Empress Dock

Southampton

Hants SO14 3ZH

1) Introduction

In our first paper (Quartly *et al.* 2001) we discussed the importance of measuring rainfall at sea, and the different *in situ* techniques available. Here we examine the various satellite-based remote-sensing techniques, since only such systems can provide near-global measurements of rain on a frequent basis. The various techniques span the electromagnetic spectrum from microwave to infra-red and visible, and also include active as well as passive sensing systems. None of the sensors measure individual raindrops, but rather the bulk properties of the rain or the storm system bearing it. Below we discuss each technique in turn.

2) Infra-red sensors

From a fixed position 35,600 km above the equator, geostationary satellites such as *Meteosat* give frequent coverage of one face of the Earth. Infra-red sensors (typically operating at wavelengths between 1 and 12 μm) observe the brightness of individual pixels on the Earth's surface, and from such observations determine the temperature of the emitting surface. This may often correspond to land or ocean, but when thick clouds are present, the measurement will correspond to the cloud top temperatures (see Fig. 1). The temperature at the top of deep convective clouds is typically 40 degrees below freezing, and thus readily distinguished from open ocean temperatures. Richards and Arkin (1981) introduced the idea of a precipitation index based on the fraction of a region covered by cloud top temperatures below a certain threshold (such as 235 K). This "observation" is not of the rain itself, but of storm systems *likely* to bear rain. Consequently the correlation between infra-red estimates of rain and ground-truth measurements of actual rain is only moderate when individual infra-red pixels are considered; much higher correlations are obtained when rain rates are averaged over large areas e.g. $2.5^\circ \times 2.5^\circ$ (Ebert and Manton 1998). It was subsequently noted that the optimum threshold varied with location, being some 15 K colder in mid-latitudes than the tropics (Arkin and Meisner 1987).

Geostationary satellites have an adequate resolution (4 km) directly below them, but this degrades considerably as their view approaches the Earth's limb. Consequently four satellites are required to cover all longitudes, and the high latitude oceans remain unobserved. A different sampling scenario may be achieved from an orbit only ~800 km up, which takes the satellite near both poles. The lower orbit provides a resolution of about 1 km, allowing more detailed images of rain systems. The disadvantage of such polar-orbiting satellites is that they cannot offer frequent (e.g. hourly) observations of particular locations, as the Earth rotates beneath them.

A variation of this technique incorporates measurements of albedo (the reflectance of visible light by clouds) to aid in the identification of different cloud types and thus in the inference of rain rate.

3) Passive microwave sensors

Alternatively one can sense rain systems in the microwave band of the electromagnetic spectrum. In simple terms, raindrops and ice particles can both scatter upwelling radiation from the Earth's surface (reducing the intensity reaching the spaceborne sensors) or augment it through their own emissions. The net effect depends upon the microwave frequencies under consideration, the background surface type and the size and nature of the hydrometeors.

Upwelling radiation at high microwave frequencies (50-100 GHz) is scattered by raining systems, leading to a reduction in the observed "brightness temperature" of the Earth's surface. It is, in fact, the ice particles within the cloud which are the dominant scatterers, and the number density of these tends to be much higher for terrestrial storms than those at sea. Thus scattering techniques provide an "indirect" measure of rainfall, with the relationship between observed brightness temperature and rainfall involving empirically-determined coefficients that are different over land and ocean, and vary with season and climate (Wilheit *et al.* 1991).

Rain estimation techniques using low microwave frequencies (10-30 GHz) are based upon the absorption/emission properties of the actual raindrops. The surface of the sea has a low emissivity and provides a weak source of polarized background emissions. Raindrops, on the other hand, are much more effective emitters, and produce V- and H-polarizations of similar intensity. The emissions increase with column density of raindrops. However, as the rain rates increase, scattering by the uppermost raindrops becomes significant. At yet higher rain rates, the detected emissions come from the higher (and cooler) part of the rain column. The result is that the observed brightness temperatures reach a maximum level and then decrease (see Fig. 2). A simple inversion from brightness temperature to rain rate is thus not possible in general with observations at a single frequency, but can be achieved using a number of different frequencies (Ferraro and Marks, 1995). Note that such a rain detection method is not applicable over land, where the surface emissions are much greater.

4) Active microwave sensors

When we look at active microwave systems, there are again two principle techniques — reflectance and attenuation. The Precipitation Radar (PR) on the TRMM satellite is the first instrument designed to measure the reflectivity of rain from space. In essence, the technique is similar to that of land-based rain radars; short pulses are transmitted at microwave frequencies, and the time delay and strength of the echo gives the distance and intensity of the rain. The differences are that the nearest rain is about 350 km away from the sensor, and that there is no rotating dish, so scanning must be achieved by electronic steering. The PR surveys a swath of width 220 km at a resolution of ~ 4.3 km (Kummerow *et al.* 1998). Furthermore, it is unique among the spaceborne systems in that it gives information on the vertical distribution of rain, with a height resolution of 250 m. The strongest signal comes from the so-called "bright band" of partially-melted hydrometeors near the base of the cloud. Thus any calculation of the reflectivity of the rain has to make allowance from the fraction of signal lost by attenuation in the bright band.

The alternative technique is to measure the fraction of the incident energy that passes right through the rain system, and hence infer the total attenuation of the rain system. In practice this means the signal has to progress vertically down through the rain, reflect off the Earth's surface, and return up through the rain to the satellite. One of the key problems with this technique is that in order to determine the attenuation effect of rain at a location, one has to know the strength of the sea surface reflectance, which varies according to the prevailing wind conditions.

The Surface Reference Technique (SRT) relies on identifying neighbouring pixels that are unaffected by rain; if they are close it can be assumed that the sea surface roughness (principally determined by the wind) is the same at the two locations. The PR uses this to provide a column-averaged rain rate, which can be a constraint on the recovery of information from the reflectance method. An improvement on this is the Dual-frequency Surface Reference Technique (DSRT), which makes use of the signal from radio pulses at a second frequency that is little affected by rain. This second frequency gives an independent measure of the sea surface reflectance. The gain from this method is illustrated in Fig. 3, using data from the TOPEX altimeter (Quartly *et al.* 1996, 1999). The black dashed line shows the surface roughness observed by C-band (5.3 GHz), but rescaled to show the value to be expected at K_u -band (13.6 GHz). The actual K_u -band observations, shown by the solid grey line, indicate two regions (27.4°N and 30°-34°N) where there is an additional effect of attenuation by raindrops, causing a discrepancy between the two lines. Both the SRT and the DSRT are sensitive to the attenuation in the bright band, and, in order to infer rain rate, require information on the height of the rain column. This could be acquired from coincident passive microwave sensors (Wilheit *et al.* 1991).

5) Production of global climatologies

The various techniques outlined above can be used to provide global climatologies as illustrated in Fig. 4. All sensors produce roughly the same geographical patterns — showing the Inter Tropical and South Pacific Convergence Zones, as well as mid-latitude storm tracks — however the rain magnitude estimates for each region vary between techniques. The Global Precipitation Climatology Project (GPCP) is a major international initiative to combine the data from different sensors. To-date it has concentrated on those datasets of long-standing — terrestrial rain gauges, infra-red measurements from geostationary satellites and passive microwave measurements from the SSM/I instruments.

The Tropical Rainfall Measuring Mission (TRMM) satellite launched in 1997 brings a number of dedicated sensors to bear on the task, albeit just in tropical latitudes. The suite of instruments on-board provide rainfall estimates through a number of active and passive microwave techniques, but to-date climatologies based on these differ by up to 30% (Kummerow *et al.* 2000).

One of the continuing challenges is to understand better the assumptions and errors in each of the techniques discussed above, especially noting that some will vary regionally according to the typical size of active rain cells and the relative occurrence of convective and stratiform systems. In high latitudes there is also the need to record accurately the precipitation occurring as hail or snow, which are not detected well by some techniques. The disagreements between the various climatologies are greatest in the mid- and high-latitudes, with even some using the same raw data differing by more than a factor of two according to the assumptions used (Adler *et al.*, 2001).

The latest generation of global forecasting models contain microphysical schemes that parametrise cloud drops and rainfall. One challenge is to develop a model that can assimilate rainfall observations. The other challenge, since rain varies on such short spatial and temporal scales, is to make sufficient measurements to sample all the major rain events. This is being addressed by the Global Precipitation Mission (Flaming *et al.* 2001) which proposes to have an accurate radar in a polar orbit, plus a number of subsidiary "drones" improving the sampling through lower-cost passive microwave sensors.

References

- Adler, R. F., Kidd, C., Petty, G., Morissey, M. and Goodman, H. M. (2001) Intercomparison of global precipitation products: The third precipitation intercomparison project (PIP-3). *Bull. Am. Meteor. Soc.* **82**, pp. 1377-1396.
- Arkin, P. A. and Meisner, B. N. (1987) The relationship between large-scale convective rainfall and cold cloud over the western hemisphere during 1982-1984. *Mon. Wea. Rev.*, **115**, pp. 51-74.
- Ebert, E. E. and Manton, M. J. (1998) Performance of satellite rainfall estimation algorithms during TOGA COARE. *J. Atmos. Sciences*, **55**, pp. 1537-1557.
- Ferraro, R. R. and Marks, G. F. (1995) The development of SSM/I rain-rate retrieval algorithms using ground-based radar measurements. *J. Atmos. Oceanic Technol.*, **12**, pp. 755-770.
- Flaming, G.M., Adams, W. J., Neeck, S. P. and Smith, E. A. (2001) Planning for Global Precipitation Measurement. *Proc. of IGARSS' 2001 (13th-17th July 2001, Sydney)* 3pp.
- Huffman, G. J., Adler, R. F., Arkin, P., Chang, A., Ferraro, R., Gruber, A., Janowiak, J., McNab, A., Rudolf, B. and Schneider, U. (1997) The Global Precipitation Climatology Project (GPCP) combined precipitation dataset. *Bull. Am. Meteor. Soc.* **78**, pp. 5-20.
- Kummerow, C., Barnes, W., Kozu, T., Shiue, J. and Simpson, J. (1998) The Tropical Rainfall Measuring Mission (TRMM) sensor package. *J. Atmos. Oceanic Technol.*, **15**, pp. 809-817.
- Kummerow, C., Simpson, J., Thiele, O., Barnes, W., Chang, A. T. C. and coauthors, (2000) The status of the Tropical Rainfall Measuring Mission (TRMM) after two years in orbit. *J. Applied Meteor.*, **39**, pp. 1965-1982.
- Quartly, G. D., Guymer, T. H. and Birch, K. G. (2001) Measuring rainfall at sea. I. In situ sensors (submitted to *Weather*)
- Quartly, G. D., Guymer, T. H. and Srokosz, M. A. (1996) The effects of rain on Topex radar altimeter data. *J. Atmos. Oceanic Technol.*, **13**, pp. 1209-1229.
- Quartly, G. D., Srokosz, M. A. and Guymer, T. H. (1999) Global precipitation statistics from dual-frequency TOPEX altimetry. *J. Geophys. Res.*, **104**, pp. 31489-31516.
- Richards, F. and Arkin, P. A. (1981) On the relationship between satellite-observed cloud cover and precipitation. *Mon. Wea. Rev.*, **109**, pp. 1081-1093.
- Spencer, R. W., Goodman, H. M. and Hood, R. E. (1989) Precipitation retrieval over land and ocean with the SSM/I: Identification and characteristics of the scattering signal. *J. Atmos. Oceanic Technol.*, **6**, pp. 254-273.

Wilheit, T. T., Chang, A. T. C. and Chiu, L. S. (1991) Retrieval of monthly rainfall indices from microwave radiometric measurements using probability distribution functions. *J. Atmos. Oceanic Technol.*, **8**, pp. 118-136.

Figures

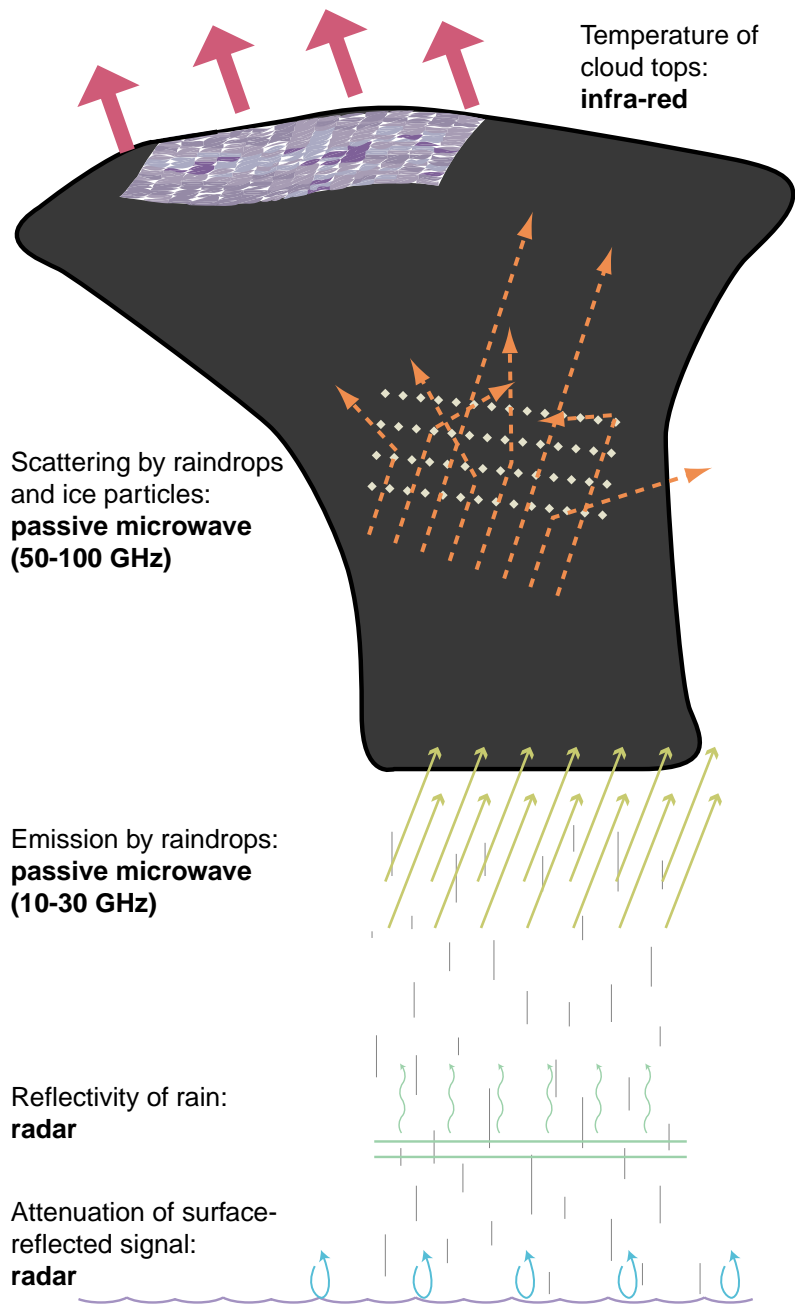


Fig. 1. Schematic of a storm cloud, and the dominant physical processes observed by different remote-sensing techniques.

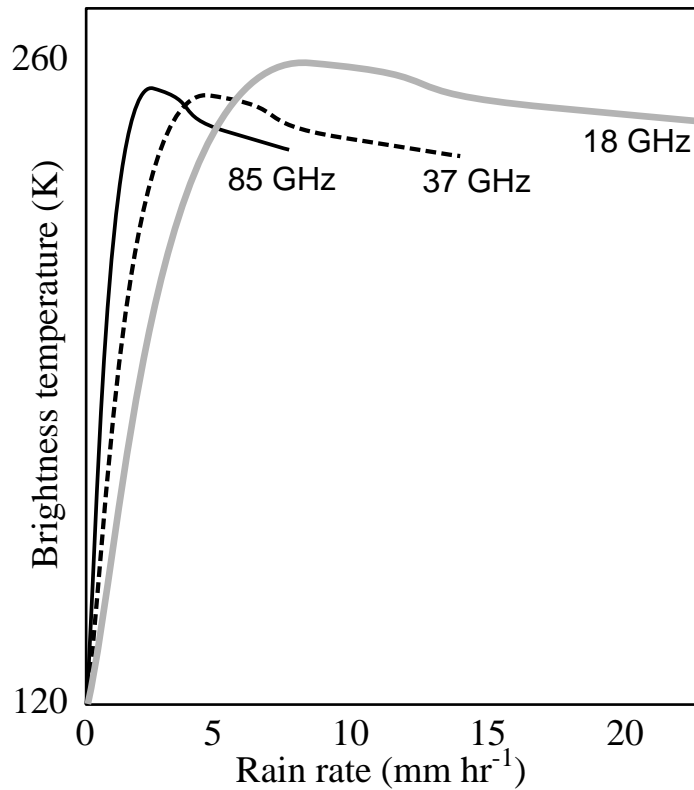


Fig. 2 Schematic of the changes in microwave brightness temperature with oceanic rain rate (after Spencer et al., 1989).

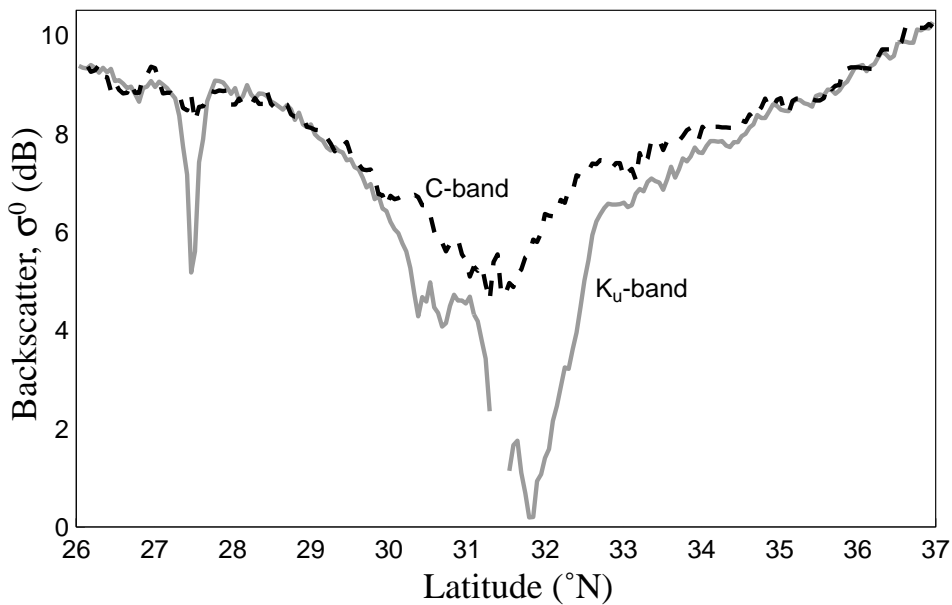
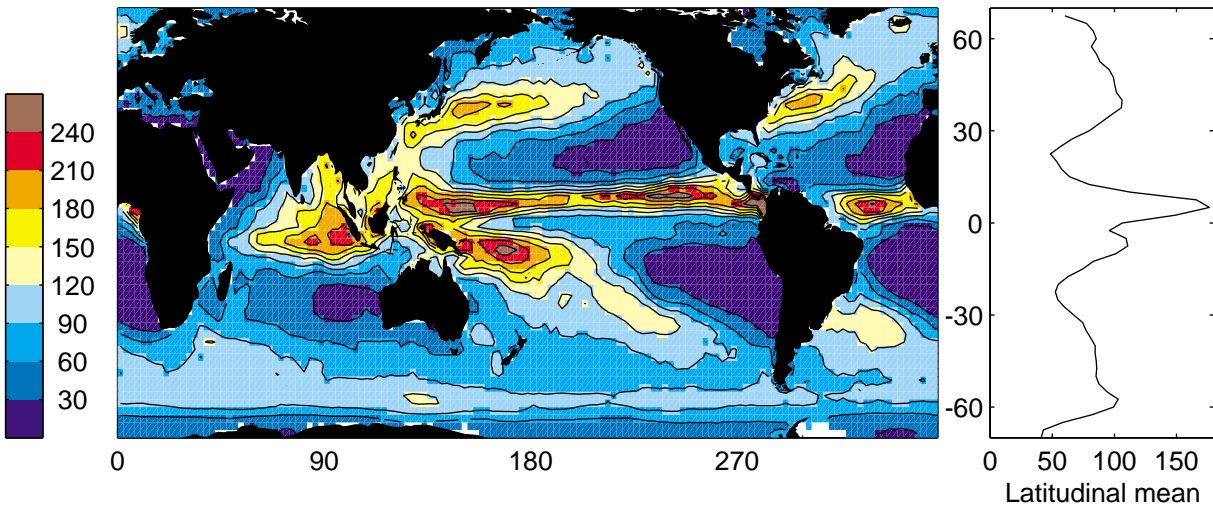


Fig. 3. Section of surface reflectivity (σ^0) across a typhoon in the N. Pacific (from Quartly et al., 1996). The K_u -band values are affected by both changes of the sea surface and attenuation by atmospheric liquid water; C-band values (shown after an empirical rescale) reflect only changes of the sea surface.

Average rainfall 1997 - 2000 (mm/month)



Average rainfall 1997 - 2000 (mm/month)

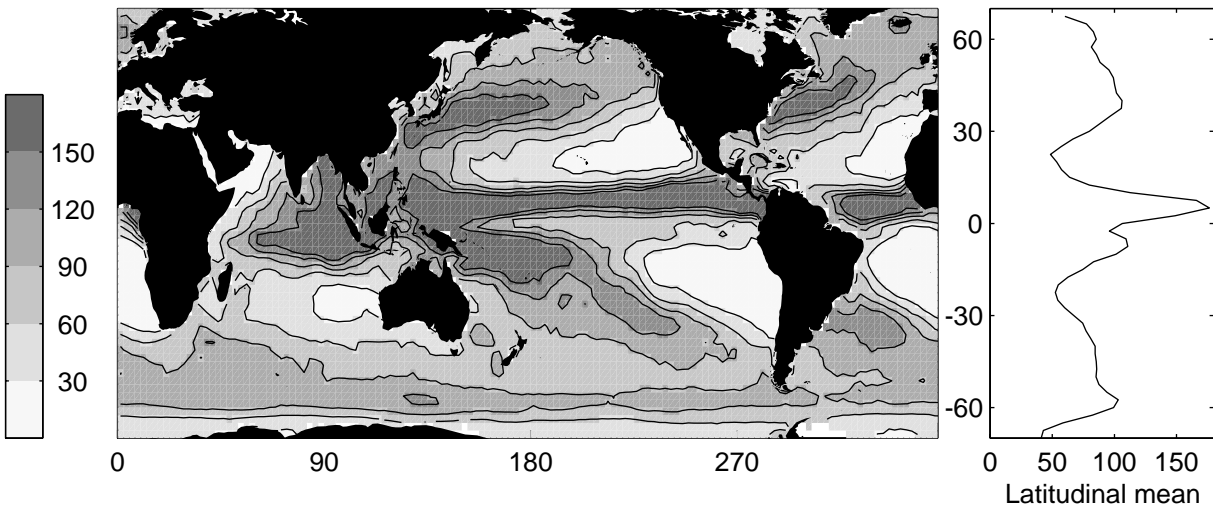


Fig. 4 Annual average rain rate from the GPCP dataset, plus latitudinal mean. (Data from Huffman et al., 1997)